Chapter 10

Determining the Trifocal tensor

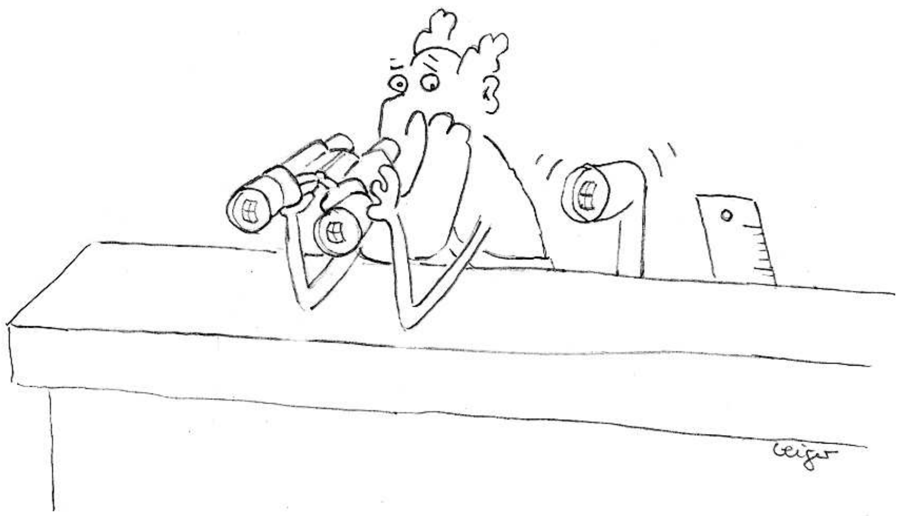

In this chapter, we work with triples of images from which triplets of corresponding features — points or lines — have been extracted. As with the two-view case 7.2, these features allow for the estimation of Trifocal geometry. The various methods to do so and their properties are discussed hereafter. Note that estimating the Trifocal tensor is still a quite hot research topic at the time of this writing and some problems are still waiting for a satisfactory solution. The material presented in this chapter is thus more a snapshot of the current state of the art than a definitive treaty on the problem.

Throughout this chapter, the tensorial notation is adopted. Points and lines will be denoted by the letters $\mathbf{m}$ and $\mathbf{l}$ respectively. An element will be noted as $\mathbf{f}$, $\mathbf{f}'$ or $\mathbf{f}''$ whenever it is associated to the first, the second or the third image respectively. The shorthand notation $\boldsymbol{\mathcal{T}}$ will be used for $\boldsymbol{\mathcal{T}}_1$ and the 27 coefficients of $\boldsymbol{\mathcal{T}}$ will be denoted by $\mathcal{T}_w^{uv}$, with reference to figure 9.8. Let the projective coordinates of a point $\mathbf{m}$ be denoted by $\left[m^1, m^2, m^3\right]^T$ and those of a line $\mathbf{l}$ by $[l_1, l_2, l_3]^T$. We use the Levi-Civita tensor defined in chapter 4, proposition 4.29 to express cross-products as:

$$l_i = \epsilon_{ijk} m'^j m''^k \equiv \sum_{j,k} \epsilon_{ijk} m'^j m''^k \qquad \mathbf{l} = \mathbf{m}' \times \mathbf{m}'' \tag{10.1}$$

10.1 The linear algorithm

As for Fundamental matrices 7.2, the simplest method to obtain the Trifocal tensor is to solve a linear system of equations. The basic idea [135, 322] is to neglect all the various Trifocal constraints and take all the 27 coefficients of the Trifocal tensor as unknowns. This yields a method which is very fast and easy to implement, but which gives tensors that do not satisfy the constraints of Trifocal tensors (see [112] and sections 9.4 and 9.5).

In this section, this algorithm and the refinements that are practically needed to make it effective are presented. Some typical results obtained with this method will be shown and used to illustrate its shortcomings.

10.1.1 Normalization again!

As for the estimation of the Fundamental matrix, the Trifocal tensor deals with projective coordinates whose order of magnitude are very different as seen in section 7.2.1 which results in poor numerical conditionning of the matrices that are involved in the linear algorithm: As it will be seen in the forthcoming sections, the entries of the matrices are products of three coordinates. Thus, a one order of magnitude discrepancy is transformed in a three order of magnitude in the estimation matrix. For this reason, the problem is even worse for the Trifocal tensor than for Fundamental matrices and normalizing the input data is mandatory.

The normalization of each image feature is the same as the one described for the Fundamental matrix. However, with the Trifocal tensor estimations, we have to take into account not only of points but also of lines. Defining a normalization for data containing lines and points is not straightforward (because the coordinates of points and lines are of different nature but a single normalization is wanted). The way this difficulty has been dealt with here is to consider that, even though the Trifocal tensor deals with lines, the image measurements are always line segments. One way to make those line segments participate to the computation of the normalization transformation is to take account only of their end-points. With this assumption, the normalization computation can be done for each image exactly as described in section 7.2.1 and gives three affine transformations $\mathbf{H}$, $\mathbf{H}'$, $\mathbf{H}''$ for the three images respectively: these define a new system of coordinates for each image[1]:

$$\widehat{\mathbf{l}} = \mathbf{H}\mathbf{l}\,, \quad \widehat{\mathbf{l}'} = \mathbf{H}'\mathbf{l}'\,, \quad \widehat{\mathbf{l}''} = \mathbf{H}''\mathbf{l}''\,.$$

Assuming that $\widehat{\boldsymbol{\mathcal{T}}}$ is the Trifocal tensor estimated using the normalized coordinate system for each image, we are interested in recovering the Trifocal tensor $\boldsymbol{\mathcal{T}}$ relating the images equipped with their original coordinate systems.

$$\begin{aligned} \widehat{\mathbf{l}} = \mathbf{H}\mathbf{l} &= \mathbf{H}\boldsymbol{\mathcal{T}}(\mathbf{l}', \mathbf{l}'') \\ &= \widehat{\boldsymbol{\mathcal{T}}}(\widehat{\mathbf{l}'}, \widehat{\mathbf{l}''}) \\ &= \widehat{\boldsymbol{\mathcal{T}}}(\mathbf{H}'\mathbf{l}', \mathbf{H}''\mathbf{l}'') \\ &= \overline{\boldsymbol{\mathcal{T}}}(\mathbf{l}', \mathbf{l}'')\,. \end{aligned}$$

Introducing the $\mathbf{G}$ matrices as in Eq. (9.10), the last two lines of the previous formula give:

$$\overline{\mathbf{G}^i} = \mathbf{H}'^T \widehat{\mathbf{G}^i} \mathbf{H}''\,.$$

Denoting by k_i^j the coefficients of the matrix $\mathbf{H}^{-1}$ and identifying $\boldsymbol{\mathcal{T}}(\mathbf{l}', \mathbf{l}'')$ with $\mathbf{H}^{-1}\overline{\boldsymbol{\mathcal{T}}}(\mathbf{l}', \mathbf{l}'')$ for all $\mathbf{l}'$ and $\mathbf{l}''$ leads to the following formulae:

$$\mathbf{G}^i = k_i^1 \overline{\mathbf{G}^1} + k_i^2 \overline{\mathbf{G}^2} + k_i^3 \overline{\mathbf{G}^3}$$

or

$$\mathbf{G}^i = k_i^1 \mathbf{H}'^T \widehat{\mathbf{G}^1} \mathbf{H}'' + k_i^2 \mathbf{H}'^T \widehat{\mathbf{G}^2} \mathbf{H}'' + k_i^3 \mathbf{H}'^T \widehat{\mathbf{G}^3} \mathbf{H}'' \tag{10.2}$$

[1] The Trifocal tensor being an object that deals essentially with lines (see chapter 9), the affine transformations that are considered here operate on lines rather than on points.

10.1.2 The basic algorithm

Assume that there is a match $\mathbf{M}$ between features (for now, let us assume that this match can be any combination of points or lines). In each of the cases that are studied here, the Trifocal constraint can be expressed as a linear system $C(\mathbf{M}) = \mathbf{0}$. These systems, which will be detailed in further sections, can be arranged to be of the form:

$$\mathbf{U}^T\mathbf{t} = 0 \ , \tag{10.3}$$

where $\mathbf{U}$ is a $27 \times N$ matrix that is specified below for each case and where $\mathbf{t}$ is a one vector which entries are the components of the Trifocal tensor. For the rest of the discussion, we adopt the convention that $\mathcal{T}_i^{jk}$ is the $9i+3j+k-12$-th component of $\mathbf{t}$, i.e:

$$\begin{aligned}\mathbf{t} = [&\mathcal{T}_1^{11}\ \mathcal{T}_1^{12}\ \mathcal{T}_1^{13}\ \mathcal{T}_1^{21}\ \mathcal{T}_1^{22}\ \mathcal{T}_1^{23}\ \mathcal{T}_1^{31}\ \mathcal{T}_1^{32}\ \mathcal{T}_1^{33}\\ &\mathcal{T}_2^{11}\ \mathcal{T}_2^{12}\ \mathcal{T}_2^{13}\ \mathcal{T}_2^{21}\ \mathcal{T}_2^{22}\ \mathcal{T}_2^{23}\ \mathcal{T}_2^{31}\ \mathcal{T}_2^{32}\ \mathcal{T}_2^{33}\\ &\mathcal{T}_3^{11}\ \mathcal{T}_3^{12}\ \mathcal{T}_3^{13}\ \mathcal{T}_3^{21}\ \mathcal{T}_3^{22}\ \mathcal{T}_3^{23}\ \mathcal{T}_3^{31}\ \mathcal{T}_3^{32}\ \mathcal{T}_3^{33}]^T \ .\end{aligned}$$

The mapping that associates $\mathbf{t}$ to $\boldsymbol{\mathcal{T}}$ will be called $\mathcal{S}$ hereafter. Equation 10.3 is linear and homogeneous in the 27 coefficients of the tensor $\boldsymbol{\mathcal{T}}$. Thus, if we are given 26 such equations, we will be able, in general, to determine a unique solution for $\boldsymbol{\mathcal{T}}$, defined up to a scale factor. As usual, minimal configurations where only 26 equations are available are quite sensitive to noise so that more equations are used in practise to get a more robust estimation of the Trifocal tensor by looking at the least-square solution of the linear system which can be formulated as:

$$\min_{\boldsymbol{\mathcal{T}}} \sum_i C(\mathbf{M}_i)^2 \ , \tag{10.4}$$

which can be rewritten as:

$$\min_{\mathbf{t}} \|\tilde{\mathbf{U}}\mathbf{t}\|^2 \ ,$$

where $\tilde{\mathbf{U}}$ is a matrix obtained by concatenation of matrices of type $\mathbf{U}$, i.e. $\tilde{\mathbf{U}} = \left[\mathbf{U}_1^T, \ldots, \mathbf{U}_n^T\right]^T$.

As in the case of the Fundamental matrix, and since $\boldsymbol{\mathcal{T}}$ is only defined up to a global scale factor, one way to solve this system is to normalize one of the 27 coefficients to be 1 which yields a parameterization of the tensor by

26 values and to solve the normal equations associated to the least squares problem. However, the preferred way is to solve the equivalent problem:

$$\min_{\mathbf{t}} \|\tilde{\mathbf{U}}\mathbf{t}\| \quad \text{with} \quad \|\mathbf{t}\| = 1 \ , \tag{10.5}$$

whose solution is the eigenvector associated to the smallest eigenvalue of $\tilde{\mathbf{U}}^T\tilde{\mathbf{U}}$. As explained in Appendix A.1, this can be easily done by computing a singular value decomposition of the matrix $\tilde{\mathbf{U}}$. As in the Fundamental matrix case, the main advantages of this second method is that it has a better stability and that the 27 coefficients of $\boldsymbol{\mathcal{T}}$ play the same role.

The following paragraphs detail the $\mathbf{U}$ matrix and the criterion C that is minimized in each of the possible configurations of point and line matches, starting with the two most common types of matches: matches of three lines and matches of three points. Other configurations that give rise to linear equations are described as well even thought they are much less useful in practice. The table below summarizes the main results of these sections, so that the reader not interested in the details can directly go to section 10.1.3. For each admissible type of match, the number of linear equations and their rank are given (columns N and R), as well as the description of the $\mathbf{U}$ matrix corresponding to it (column Matrix). The entry C describes the symbol used to represent the number of matches of this type.

Type	N	R	Matrix	C
$(\mathbf{l}, \mathbf{l}', \mathbf{l}'')$	3	2	$\mathbf{U_{lll}} = \mathcal{S}(\epsilon^{qir} l_r l'_j l''_k)_{q\in\{1,2,3\}}$	n_{lll}
$(\mathbf{m}, \mathbf{m}', \mathbf{m}'')$	9	4	$\mathbf{U_{ppp}} = \mathcal{S}(\epsilon_{jrp}\epsilon_{ksq} m^i m'^r m''^s)_{(p,q)\in\{1,2,3\}}$	n_{ppp}
$(\mathbf{m}, \mathbf{l}', \mathbf{l}'')$	1	1	$\mathbf{U_{pll}} = \mathcal{S}(m^i l'_j l''_k)$	n_{pll}
$(\mathbf{m}, \mathbf{m}', \mathbf{l}'')$	3	2	$\mathbf{U_{ppl}} = \mathcal{S}(\epsilon_{jrp} m^i m'^r l''_k)_{p\in\{1,2,3\}}$	n_{ppl}
$(\mathbf{m}, \mathbf{l}', \mathbf{m}'')$	3	2	$\mathbf{U_{plp}} = \mathcal{S}(\epsilon_{ksq} m^i l'_j m''^s)_{q\in\{1,2,3\}}$	n_{plp}

10.1.2.1 The line-line-line configuration

Given the match $(\mathbf{l}, \mathbf{l}', \mathbf{l}'')$, by definition of the Trifocal tensor, the equation $\mathbf{l} \simeq \boldsymbol{\mathcal{T}}(\mathbf{l}', \mathbf{l}'')$ is satisfied. Consequently, a system of 3 linear equations in the coefficients of $\boldsymbol{\mathcal{T}}$ can be written: $\boldsymbol{\mathcal{T}}(\mathbf{l}', \mathbf{l}'') \times \mathbf{l} = 0$. Because of the cross-product, this system is of rank 2.

$$C_{lll}(\mathbf{l}, \mathbf{l}', \mathbf{l}'') = \boldsymbol{\mathcal{T}}(\mathbf{l}', \mathbf{l}'') \times \mathbf{l} = \epsilon^{qir} l_r l'_j l''_k \mathcal{T}_i^{jk} \ .$$

The corresponding $\mathbf{U_{lll}}$ matrix is:

$$\begin{aligned}\mathbf{U_{lll}}(\mathbf{l},\mathbf{l}',\mathbf{l}'') &= \mathcal{S}(\epsilon^{qir} l_r l'_j l''_k)_{q\in\{1,2,3\}} \\ &= \begin{bmatrix} \mathbf{0}_{1\times 9} & -l_3\mathbf{K}_{ll}(\mathbf{l}',\mathbf{l}'') & l_2\mathbf{K}_{ll}(\mathbf{l}',\mathbf{l}'') \\ l_3\mathbf{K}_{ll}(\mathbf{l}',\mathbf{l}'') & \mathbf{0}_{1\times 9} & -l_1\mathbf{K}_{ll}(\mathbf{l}',\mathbf{l}'') \\ -l_2\mathbf{K}_{ll}(\mathbf{l}',\mathbf{l}'') & l_1\mathbf{K}_{ll}(\mathbf{l}',\mathbf{l}'') & \mathbf{0}_{1\times 9} \end{bmatrix} ,\end{aligned} \tag{10.6}$$

where $\mathbf{K}_{ll}(\mathbf{l}',\mathbf{l}'') = \begin{bmatrix} l'_1 l''_1 & l'_1 l''_2 & l'_1 l''_3 & l'_2 l''_1 & l'_2 l''_2 & l'_2 l''_3 & l'_3 l''_1 & l'_3 l''_2 & l'_3 l''_3 \end{bmatrix}$. The number of such line-line-line configurations is called n_{lll} hereafter.

10.1.2.2 The point-point-point configuration

Given a point match $(\mathbf{m},\mathbf{m}',\mathbf{m}'')$, the criterion C_{ppp} is obtained by considering all pairs of lines such that the first belongs to the pencil of lines centered at $\mathbf{m}'$ and the second belongs to the pencil of lines centered at $\mathbf{m}''$. This is equivalent to consider two arbitrary points $\mathbf{x}'$ and $\mathbf{x}''$ in images 2 and 3 respectively. Then, $\mathbf{m}'\times\mathbf{x}'$ represents an arbitrary line of image 2 passing through the point $\mathbf{m}'$ and similarly $\mathbf{m}''\times\mathbf{x}''$ represents an arbitrary line of image 2 passing through the point $\mathbf{m}''$. Consequently, $\boldsymbol{\mathcal{T}}(\mathbf{m}'\times\mathbf{x}',\mathbf{m}''\times\mathbf{x}'')$ is a line of image 1 containing the point $\mathbf{m}$ and $\boldsymbol{\mathcal{T}}$ obeys the linear equation:

$$Eq_{ppp}(\mathbf{x}',\mathbf{x}'') = \mathbf{m}^T\boldsymbol{\mathcal{T}}(\mathbf{m}'\times\mathbf{x}',\mathbf{m}''\times\mathbf{x}'') = m^i\mathcal{T}_i^{jk}\epsilon_{jrp}m'^r x'^p \epsilon_{ksq}m''^s x''^q = 0 \ .$$

Since this equation is true for all points $\mathbf{x}'$ and $\mathbf{x}''$ and since the equation is linear in the coordinates of each of these two points, it is sufficient, in theory, to choose them in the projective bases of their respective images.

$$\begin{aligned} C_{ppp}(\mathbf{m},\mathbf{m}',\mathbf{m}'') &= \epsilon_{jrp}\epsilon_{ksq}\mathcal{T}_i^{jk}m^i m'^r m''^s \\ &= Eq_{ppp}(\boldsymbol{\varepsilon}^p,\,\boldsymbol{\varepsilon}^q) \end{aligned} \quad , \quad (p,q)\in\{1,2,3\} \ ,$$

where $\boldsymbol{\varepsilon}^i$, $i = 1\ldots 3$ is the canonical projective basis of image 2 and 3 (for simplicity the two basis have been identified here). $C_{ppp}(\mathbf{m},\mathbf{m}',\mathbf{m}'')$ is thus a system of 9 linear equations. Since each pencil of lines is of linear dimension 2, the system is of rank[2] 4, and its matrix $\mathbf{U_{ppp}}$ is defined by:

$$\begin{aligned}\mathbf{U_{ppp}}(\mathbf{m},\mathbf{m}',\mathbf{m}'') &= \mathcal{S}(\epsilon_{jrp}\epsilon_{ksq}m^i m'^r m''^s)_{(p,q)\in\{1,2,3\}^2} \\ &= \begin{bmatrix} m^1\mathbf{K_{pp}}(\mathbf{m}',\mathbf{m}'') & m^2\mathbf{K_{pp}}(\mathbf{m}',\mathbf{m}'') & m^3\mathbf{K_{pp}}(\mathbf{m}',\mathbf{m}'') \end{bmatrix} ,\end{aligned}$$

[2] All the 9 equations are necessary though, in order to obtain a rank 4 system for all choices of $\mathbf{m}'$ and $\mathbf{m}''$.

with

$$\mathbf{K_{pp}}(\mathbf{m}', \mathbf{m}'') = \begin{bmatrix} \mathbf{0}_{3\times3} & m'^3[\mathbf{m}'']_\times & -m'^2[\mathbf{m}'']_\times \\ -m'^3[\mathbf{m}'']_\times & \mathbf{0}_{3\times3} & m'^1[\mathbf{m}'']_\times \\ m'^2[\mathbf{m}'']_\times & -m'^1[\mathbf{m}'']_\times & \mathbf{0}_{3\times3} \end{bmatrix},$$

These 9 equations are often reffered to as the trilinearities associated with

the match $(\mathbf{m}, \mathbf{m}', \mathbf{m}'')$. In the remaining of this section, n_{ppp} will represent the number of such of point-point-point configurations.

10.1.2.3 The point-line-line configuration

Given the match $(\mathbf{m}, \mathbf{l}', \mathbf{l}'')$, by definition of the Trifocal tensor, $\boldsymbol{\mathcal{T}}(\mathbf{l}', \mathbf{l}'')$ is a line of image 1 passing through the point $\mathbf{m}$. The criterion C_{pll} is thus restricted to a single linear equation:

$$C_{pll} = \mathbf{m}^T \boldsymbol{\mathcal{T}}(\mathbf{l}', \mathbf{l}'') = m^i \mathcal{T}_i^{jk} l'_j l''_k \,, \tag{10.7}$$

with the corresponding $\mathbf{U_{pll}}$ matrix:

$$\begin{aligned} \mathbf{U_{pll}}(\mathbf{m}, \mathbf{l}', \mathbf{l}'') &= \mathcal{S}(m^i l'_j l''_k) \\ &= \begin{bmatrix} m^1 \mathbf{K}_{ll}(\mathbf{l}', \mathbf{l}'') & m^2 \mathbf{K}_{ll}(\mathbf{l}', \mathbf{l}'') & m^3 \mathbf{K}_{ll}(\mathbf{l}', \mathbf{l}'') \end{bmatrix}, \end{aligned}$$

with $\mathbf{K}_{ll}(\mathbf{l}', \mathbf{l}'')$ defined as in section 10.1.2.1.
The number of such point-line-line configurations is called n_{pll} hereafter.

10.1.2.4 The point-point-line configuration

Given the match $(\mathbf{m}, \mathbf{m}', \mathbf{l}'')$, the criterion C_{ppl} is obtained as in section 10.1.2.2 by considering all the lines belonging to the pencil centered at $\mathbf{m}'$. This is again equivalent to consider one arbitrary point $\mathbf{x}'$ in images 2. Then, $\mathbf{m}' \times \mathbf{x}'$ represents an arbitrary line of image 2 passing through the point $\mathbf{m}'$. Consequently, $\boldsymbol{\mathcal{T}}(\mathbf{m}' \times \mathbf{x}', \mathbf{l}'')$ is a line of image 1 containing the point $\mathbf{m}$ and $\boldsymbol{\mathcal{T}}$ obeys the linear equation:

$$Eq_{ppl}(\mathbf{x}') = \mathbf{m}^T \boldsymbol{\mathcal{T}}(\mathbf{m}' \times \mathbf{x}', \mathbf{l}'') = m^i \mathcal{T}_i^{jk} \epsilon_{jrp} m'^r x'^p l''_k = 0 \,.$$

This equation being linear and true for all points $\mathbf{x}'$, it is sufficient to choose this point in the projective basis of image 2.

$$\begin{array}{rcl} C_{ppl}(\mathbf{m},\mathbf{m}',\mathbf{l}'') & = & m^i \mathcal{T}_i^{jk} \epsilon_{jrp} m'^r l''_k \\ & = & Eq_{ppl}(\boldsymbol{\varepsilon}^p) \end{array} \quad , \quad p \in \{1,2,3\} \; ,$$

where $\boldsymbol{\varepsilon}^p$, $p = 1 \dots 3$ is the canonical projective basis of image 2. $C_{ppl}(\mathbf{m},\mathbf{m}',\mathbf{l}'')$ is thus a system of 3 linear equations. Since a pencil of lines is of dimension 2, this system is of rank 2, and its matrix $\mathbf{U_{ppl}}$ is defined by:

$$\begin{array}{rcl} \mathbf{U_{ppl}}(\mathbf{m},\mathbf{m}',\mathbf{l}'') & = & \mathcal{S}(\epsilon_{jrp} m^i m'^r l''_k)_{p\in\{1,2,3\}} \\ & = & \begin{bmatrix} m^1 \mathbf{K_{pl}}(\mathbf{m}',\mathbf{l}'') & m^2 \mathbf{K_{pl}}(\mathbf{m}',\mathbf{l}'') & m^3 \mathbf{K_{pl}}(\mathbf{m}',\mathbf{l}'') \end{bmatrix} \; , \end{array}$$

with

$$\mathbf{K_{pl}}(\mathbf{m}',\mathbf{l}'') = \begin{bmatrix} \mathbf{0}_{1\times 3} & m'^3 \mathbf{l}''^T & -m'^2 \mathbf{l}''^T \\ -m'^3 \mathbf{l}''^T & \mathbf{0}_{1\times 3} & m'^1 \mathbf{l}''^T \\ m'^2 \mathbf{l}''^T & -m'^1 \mathbf{l}''^T & \mathbf{0}_{1\times 3} \end{bmatrix} ,$$

The number of such configurations is called n_{ppl}.

10.1.2.5 The point-line-point configuration

Given the match $(\mathbf{m},\mathbf{l}',\mathbf{m}'')$, the reasoning to obtain the criterion C_{ppl} is very similar to the point-point-line case described in the previous section and it is left to the reader as an exercise to verify that:

$$\begin{array}{rcl} \mathbf{U_{plp}}(\mathbf{m},\ \mathbf{l}',\mathbf{m}'') & = & \mathcal{S}(\epsilon_{ksq} m^i l'_j m''^s)_{q\in\{1,2,3\}} \\ & = & \begin{bmatrix} m^1 \mathbf{K_{lp}}(\mathbf{l}',\mathbf{m}'') & m^2 \mathbf{K_{lp}}(\mathbf{l}',\mathbf{m}'') & m^3 \mathbf{K_{lp}}(\mathbf{l}',\mathbf{m}'') \end{bmatrix} \; , \end{array}$$

with

$$\mathbf{K_{lp}}(\mathbf{l}',\mathbf{m}'') = \begin{bmatrix} l'_1 \mathbf{L_p}(\mathbf{m}'') & l'_2 \mathbf{L_p}(\mathbf{m}'') & l'_3 \mathbf{L_p}(\mathbf{m}'') \end{bmatrix} ,$$

The number of such configurations is called n_{plp}.

10.1.3 Discussion

Combining the elements of the previous sections, it is easy to implement a linear algorithm for the estimation of the Trifocal tensor using standard linear algebra tools. The same algorithm can deal with matches made out of various combinations of points and lines. However, the careful reader must have noticed that three types of matches have not been considered in the previous list: indeed the line-point-line or line-line-point or line-point-point type of match *do not* contribute to any linear equation. This is because the primitive observed in image 1 in those three cases is a line $\mathbf{l}$ and the one predicted from the data in images 2 and 3 is a point. We saw in the previous sections that a point information must first be converted into an information about a pencil of lines before it can be handeled by the Trifocal tensor. Thus, the question that has to be answered in image 1 is "Is $\mathbf{l}$ a line belonging to some given pencil of lines ?". Unfortunately, the algebraic test corresponding to this question is of degree 2 in the components of $\boldsymbol{\mathcal{T}}$, thus no linear equations are available.

We have seen that the Trifocal tensor is defined by 26 coefficients. Given the ranks of the elementary matrices described in the previous sections, it is thus determined by the linear algorithm as soon as $n_{pll}+2n_{lll}+2n_{ppl}+2n_{plp}+4n_{ppp} \geq 26$. In the extreme situations where only one type of primitive is used, the minimal number of features required for the linear algorithm is either 7 points or 13 lines matched across the three images.

10.1.4 Some results

We present results to help the reader evaluate the quality of the methods used to estimate the Trifocal tensor. We use two different types of input.

10.1.4.1 Synthetic experiments

First, we use a set of ideal data points for which the result is known. These data are used to gather statistical results about the linear estimation process. For each noise level (gaussian noise), noise is added to the ideal points 1000 times and the linear estimation procedure is run. Statistics are gathered from all these samples. Figure 10.1 shows the three set of points that are used as input. Notice that, even though the data are perfect, the geometrical situation of the cameras is realistic as it stems from a trinocular stereo setup.

To characterize the quality of the results, we first plot the statistics related to the smallest singular values. Figure 10.2 shows two plots. The left plot shows the evolution of the smallest singular value with respect to the (Gaussian) noise level. As it can be expected, the minimum singular value (which reflects the average error of the linear criterion) grows linearly with the noise as well as its standard deviation. The right plot is more interesting: the displayed curves are related to the ratio of the two smallest singular values. As it can be seen, this ratio first increases linearly as well as its standard deviation, but starting at the 0.3 standard deviation noise, the behaviour of

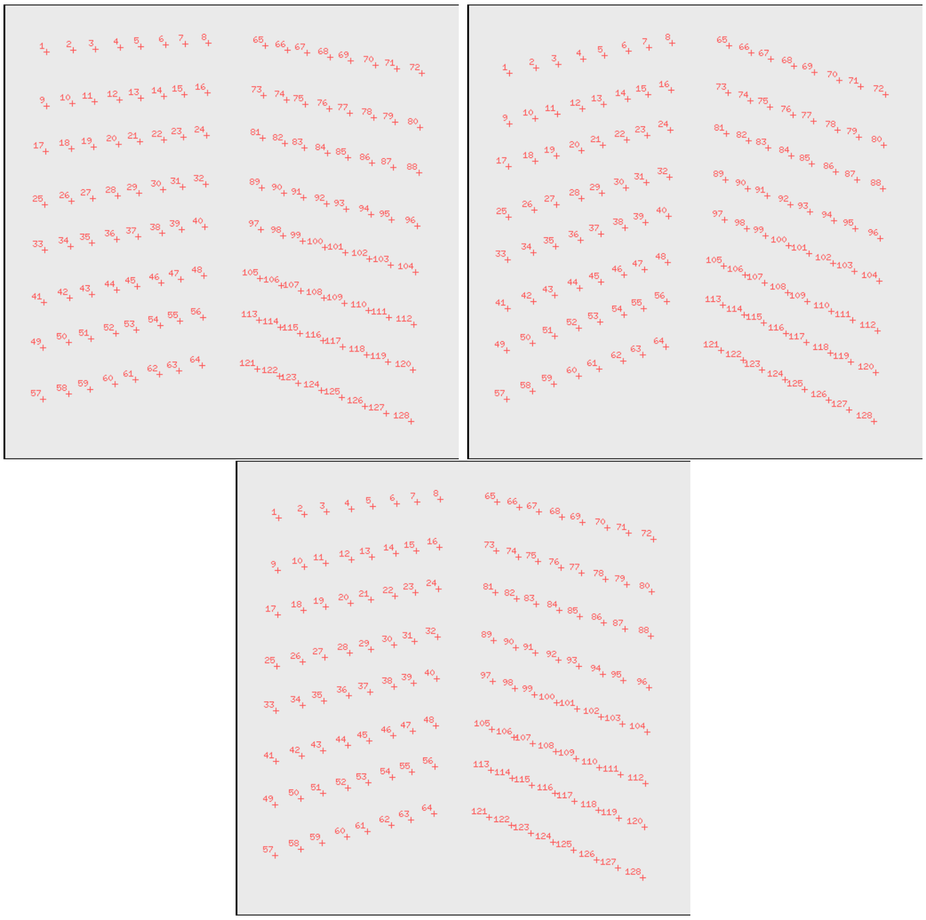

Figure 10.1: The data points used for the experiments on synthetic data.

the curve clearly changes: it starts decreasing and the standard deviation stays roughly constant. What seems to happen here is that the noise starts to hide completely the structural properties of the scene as seen from the images. Thus, the actual Trifocal tensor can no longer be recovered from the input data. In other words, what is measured in the smaller singular values is not only the Trifocal tensor but also part of the scene structure. Thus, the above algorithm is likely to produce very bad estimates in some situations. This result should be taken with care, as our data set comes from a very simple scene structure (the 3D points are scattered over two orthogonal planes) and a very particular viewing geometry (small baseline used for trinocular stereo). On the other hand, with many scenes (and particularly with urban scenes), these conditions might be a problem.

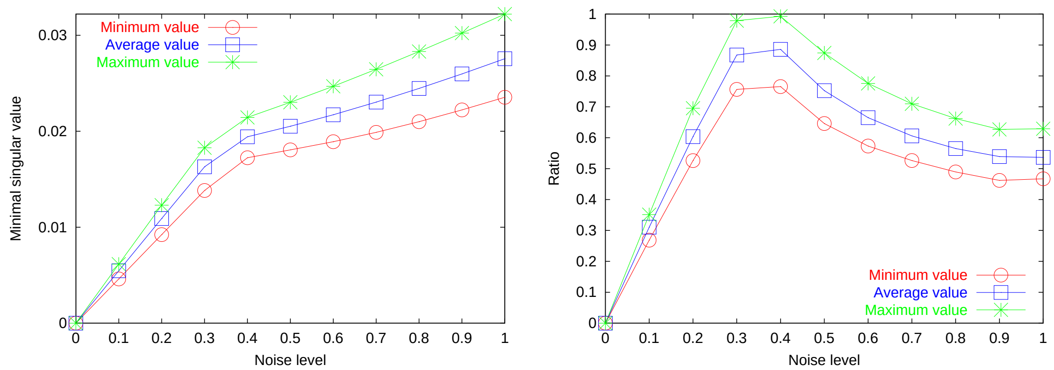

Figure 10.2: Statistics gathered over the smallest singular values. The left plot shows the value of the smallest singular value whereas the right plot shows the ratio between the two smallest singular values. In each case, the minimum, average and maximum values over the 1000 trials are shown for each noise level.

The next set of results is related to the geometric errors between the measured points in the first image and their predictions obtained by applying the Trifocal tensor to the data gathered from the other images. In figure 10.3, we show the evolutions of the average geometric errors with the noise for the solution estimated by the linear algorithm (left) and the theoretical solution (right), i.e. we apply the estimated and theoretical tensors to the noisy primitives and compute the geometric errors (more on those in section 10.5.2. Comparing those two plots, it can be seen that the linear method starts to show an unexpected behaviour at noise levels of about 0.3–0.4 standard deviation. This is in agreement with the previous results. One more interesting piece of information is the fact that the curve showing the value of the maximum average error over the 1000 trials has values (that are not shown in the plot) in the range 12–440. Comparing those with the maximum average residual of the linear method (given by the maximum value of the smallest singular values), we can see that there are some noisy situations for which the linear and the geometrical criteria behave very differently.

Fortunately, all the situations are not as difficult as the one shown in this example as we will see next with some real situations. Nonetheless, the main lessons to be learnt from this case are:

- Linear methods for estimating the Trifocal tensor can behave very badly in some situations.

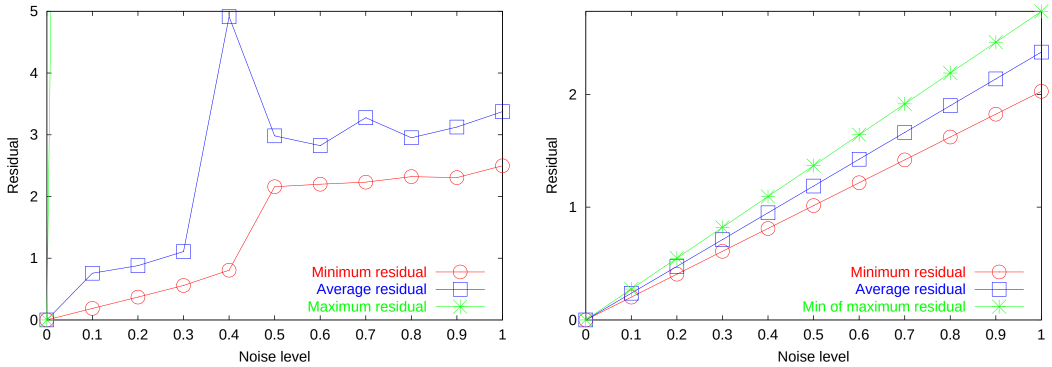

Figure 10.3: Statistics gathered over the geometric residuals. The left plot shows the values of the mean of the geometric errors obtained using the tensor obtained by the linear algorithm whereas the right plot shows the geometric errors obtained using the exact theoretical tensor. In each case, the minimum, average and maximum values of the mean residual over the 1000 trials are shown for each noise level.

- Even if they might work on average, linear methods can fail for a special noise distributions.
- Checking the quality of the obtained result is mandatory. One such test is to verify that the ratio between the two smallest singular values is small enough (one order of magnitude at least).
- The linear and the geometric criteria can have very different behaviours.

10.1.4.2 Real data experiments

We also use some real sets of images to see practically what are the sizes of the errors that we obtain from data corrupted by a typical noise. The point matches were obtained manually (clicking the points in the images without subpixel accuracy) so that points exhibit a standard level of noise and no outliers are corrupting the input. Figures 10.4, 10.5 and 10.6 show the images and the points used for these experiments. These three experiments are referred to by the names **Office**, **Library** and **Arcades**, respectively. In addition, the points of experiments **Office** and **Library** have been refined to obtain sub-pixel accuracy and have also been used: these variants are called **Office'** and **Library'**, respectiveley.

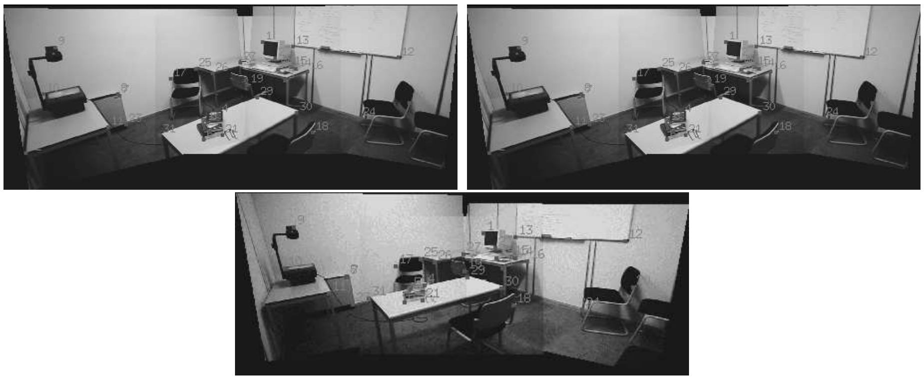

Figure 10.4: An indoor input scene, each image is a mosaic of smaller images (Courtesy **Luc Robert**, INRIA). These data correspond to the **Office** and **Office'** experiments.

	Office	Office'	Library	Library'	Arcades
Average geometric error	1.6	1.4	2.3	0.5	0.77
Maximum geometric error	4.3	3.7	9.3	2.5	2.0
Smallest singular value	$6.6e^{-3}$	$6.0e^{-3}$	$2.6e^{-3}$	$3.6e^{-4}$	$4.8e^{-3}$
Ratio	0.19	0.17	$4.4e^{-2}$	$6.3e^{-3}$	0.24

Table 10.1: Quality of the linear estimation of the Trifocal tensor with real data. For each experiment, the average and maximum error is given as well as the smallest singular value and the ratio of the two smallest singular values.

Table 10.1 gives the results obtained using the linear algorithm. From these results, one can notice various things:

- The ratio of the two smallest singular values is usually small (less than 0.3) which shows that we can have some confidence in the results.
- While the average error remains relatively low, the maximum error can be significantly higher. The experiments **Library** and **Library'** show that rounding the point coordinates can increase the residuals (geometrical or linear) significantly.

It is important to note that the tensors that have been obtained in each of these cases *do not* satisfy the Trifocal tensor constraints. This means

	Average error	Maximum Error
Image 1	0.5	2.5
Image 2	1.8	4.9
Image 3	21.1	84.9

Table 10.2: The geometric errors for the **Library'** experiment. The Trifocal tensor computed using the linear method (that gives predictions in image 1) has been used in a "change of view" operation to compute the two other Trifocal tensor associated to the three images. These tensors have then be used for prediction. The average and maximum errors between the input data points and the predicted points are shown for each image.

that the tensors that have been computed cannot be used in a change of view operation (the system being solved in a least squares fashion) and give satisfactory results. Table 10.2 gives an example of the typical poor quality of doing such a computation. These data are obtained from the **Library'** experiment, which was the most accurate case (see table 10.1). Of course, for each experiment, three Trifocal tensors can be computed but these cannot be related to each other easily.

10.2 Parameterizing the Trifocal tensor

A central tool to estimate a consistent Trifocal tensor (i.e. a tensor satisfying the Trifocal constraints described in sections 9.4 and 9.5 of chapter 9) is to have a parameterization that allows a description of the admissible Trifocal tensors. Because of the great number of constraints that have to be satisfied, parameterization of the Trifocal tensor is not as straightforward as in the Fundamental matrix case. A consequence of this is that a variety of very different parameterizations have been proposed:

- Historically, the first parameterization has been proposed by Hartley [140]. This parameterization uses 2 standard projection matrices to represent a Trifocal tensor. It is extremely elegant and quite natural but has the major drawback of not being minimal since it uses a total of 22 degrees of freedom. Thus to make the representation really effective some additional constraints which are not so natural have to be added.

- Torr and Zisserman proposed a minimal parameterization based on 6 point correspondences [371]. In this method, four of the points are used to define a canonical basis in each image, the projective coordinates of the two remaining points in those bases provide the 18 parameters that are needed. Unfortunately, a vector of 18 such parameters can represent up to three Trifocal tensors which cannot be discriminated without the use of a seventh point.

- Faugeras and Papadopoulo proposed another parameterization that is very close to the tensorial representation of the tensor and that relies directly on geometrical interpretations of the constraints that Trifocal tensors must satisfy [112]. Unfortunately, similarly to what happens with the 6-point correspondences parameterization, this parameterization is not one to one and a vector of 18 parameters represents two Trifocal tensors. Only the data can discriminate between the two candidates.

- Finally, the same authors proposed another minimal representation which is based on even less obvious geometrical properties of the Trifocal tensor that overcome the problem raised in the two previous ones [265]. At the time of this writing, this parameterization is the only one that is both minimal and one to one.

We now review each of these parameterizations.

10.2.1 The parameterization by projection matrices

Since the Trifocal tensor represents configurations of three cameras, it is natural to try to parameterize by means of projection matrices. In chapter 9, the general formula linking the Trifocal tensor to a set of three projection matrices is given by formula (9.12). However, since the Trifocal tensor is defined only up to a global collineation of the 3D space, this transform can be chosen in such a way that the first of these 3 cameras takes the standard form:

$$\boldsymbol{\mathcal{P}}_1 = \boldsymbol{\mathcal{P}}_0$$

In this same basis, the other two projection matrices take the form $\boldsymbol{\mathcal{P}}_2 = \left[\alpha_j^i\right]$ and $\boldsymbol{\mathcal{P}}_3 = \left[\beta_j^i\right]$. With these notations, the Trifocal tensor elements are given by the formula:

$$\mathcal{T}_i^{jk} = \alpha_i^j \beta_4^k - \alpha_4^j \beta_i^k \ . \tag{10.8}$$

As such this gives a parameterization of the tensor in terms of 22 parameters (as each of the projection matrix is defined only up to a scale factor). As stated in [140], this means that the jacobian of the non-linear constraints cannot have a full rank (since there is a three-dimensional set of solutions). Depending on the non-linear minimization methods this may or may not be a problem, but it is likely to have poor convergence properties, to create unstability problems, or just increase the cost of the computation. One method to remove the superfluous degrees of freedom is to remark that with the previous formulae the coefficients G^i_{jk} do not change if we replace α^i_j and β^i_j by $\alpha^i_j + \lambda_j \alpha^i_4$ and $\beta^i_j + \lambda_j \beta^i_4$, respectively: consequently, it is possible to impose an additional constraint e.g. on the α^i_j. The method that has been proposed is to impose the three linear constraints $\sum_i \alpha^i_j \alpha^i_4 = 0$, $j = 1, 2, 3$, which means that the fourth column of $\boldsymbol{\mathcal{P}}_2$ is orthogonal to all other columns[3]. Imposing these 3 constraints results in a parameterization of the Trifocal tensor with 18 parameters. A slight drawback of this method is that the parameterization is not symmetric with respect to the 3 cameras.

10.2.2 The 6-point parameterization

The six point parameterization finds its root in the study of the invariant quantities that can be defined by the observation of six points in three cameras [277]. The algorithm uses 6 points $\mathbf{M}_i, i = 1 \dots 6$ in general position in space to parameterize the Trifocal tensor. Five of those points are assigned to a 3D projective basis so that their projective coordinates can be set as follows: $\mathbf{M}_1 = [1,0,0,0]^T$, $\mathbf{M}_2 = [0,1,0,0]^T$, $\mathbf{M}_3 = [0,0,1,0]^T$, $\mathbf{M}_4 = [0,0,0,1]^T$ and $\mathbf{M}_5 = [1,1,1,1]^T$. The remaining 3D point is given the coordinates $\mathbf{M}_6 = [X, Y, Z, W]$. Similarly, the images of the first four points in each image (the image of the point $\mathbf{M}_i$ in camera j is denoted by $\mathbf{m}^j_i$) are used to define a projective basis of each image plane, ie $\mathbf{m}^j_1 = [1,0,0]^T$, $\mathbf{m}^j_2 = [0,0,1]^T$, $\mathbf{m}^j_3 = [0,0,1]^T$ and $\mathbf{m}^j_4 = [1,1,1]^T$. For each image, given the basis defined by the first 4 points, it is possible to compute the coordinates in this basis of the fifth and sixth points (it is just a matter of computing and applying an homography). Given this basis for each image, it is easy to compute the projective coordinates of the fifth and sixth image points: $\mathbf{m}^j_5 = [x^j_5, y^j_5, w^j_5]^T$ and $\mathbf{m}^j_6 = [x^j_6, y^j_6, w^j_6]^T$.

This particular choice of coordinates mandates for a very special form of the projection matrices. Using the first four points, it can be shown that they must be of the form:

[3]This also means that these columns are linearly dependent.

$$\boldsymbol{\mathcal{P}}_i = \begin{bmatrix} \alpha^i & 0 & 0 & \delta^i \\ 0 & \beta^i & 0 & \delta^i \\ 0 & 0 & \gamma^i & \delta^i \end{bmatrix}$$

Denoting by $\boldsymbol{\kappa}^i$ the vector $[\alpha^i, \beta^i, \gamma^i]^T$, the fifth point gives (because $\boldsymbol{\mathcal{P}}_i$ is defined only up to a scale factor, we can take the following equation as an algebraic equality instead of a purely projective one):

$$\boldsymbol{\kappa}^i = \mathbf{m}_5^i - \delta^i [1, 1, 1]^T \ .$$

We write the projection equation for the sixth point:

$$\mathbf{m}_6^i \times \left(\begin{bmatrix} X & 0 & 0 \\ 0 & Y & 0 \\ 0 & 0 & Z \end{bmatrix} \boldsymbol{\kappa}^i + \delta^i \begin{bmatrix} W \\ W \\ W \end{bmatrix} \right) = \mathbf{m}_6^i \times \begin{bmatrix} X x_5^i \\ Y y_5^i \\ Z w_5^i \end{bmatrix} + \delta^i \mathbf{m}_6^i \times \begin{bmatrix} W - X \\ W - Y \\ W - Z \end{bmatrix} = \mathbf{0} \ .$$

Because of the cross-product, this system has rank 2. In order to have a solution in δ^i, the two vectors of the sum must be proportional:

$$\left(\mathbf{m}_6^i \times \begin{bmatrix} X x_5^i \\ Y y_5^i \\ Z w_5^i \end{bmatrix} \right) \times \left(\mathbf{m}_6^i \times \begin{bmatrix} W - X \\ W - Y \\ W - Z \end{bmatrix} \right) = \mathbf{0} \ .$$

Expanding the cross-product yields:

$$\begin{vmatrix} x_6^i & X x_5^i & W - X \\ y_6^i & Y y_5^i & W - Y \\ w_6^i & Z w_5^i & W - Z \end{vmatrix} \mathbf{m}_6^i = \mathbf{0} \ , \text{ which implies } \begin{vmatrix} x_6^i & X x_5^i & W - X \\ y_6^i & Y y_5^i & W - Y \\ w_6^i & Z w_5^i & W - Z \end{vmatrix} = 0 \ .$$

Expanding this determinant yields:

$$\begin{array}{l} x_5^i (y_6^i - w_6^i) XW + y_5^i (w_6^i - x_6^i) YW + w_5^i (x_6^i - y_6^i) ZW + \\ x_6^i (y_5^i - w_5^i) YZ \ + y_6^i (w_5^i - x_5^i) XZ + w_6^i (x_5^i - y_5^i) XY \quad = 0 \ . \end{array}$$

This equation holds for each image, so that we get 3 linear constraints on the vector $\mathbf{u} = [XY, XZ, XW, YZ, YW, ZW]^T$. Moreover, it can be easily checked that the sum of the coefficients of the previous equation is always zero so that this system has a solution of the form:

$$\mathbf{u} = \boldsymbol{\tau} + \lambda_1 \boldsymbol{\mu} + \lambda_2 [1, 1, 1, 1, 1, 1]^T \ .$$

Looking at $\mathbf{u}$, it is clear that its components obey the following constraints: $u_1 u_6 = u_2 u_5 = u_3 u_4$. Replacing the previous formula into these constraints, yields two linear equations in λ_2.

$$\begin{aligned}
&((\mu_1-\mu_2-\mu_5+\mu_6)\lambda_1+\tau_1-\tau_2-\tau_5+\tau_6)\lambda_2+\\
&\qquad(\mu_1\mu_6-\mu_2\mu_5)\lambda_1^2+(\tau_1\mu_6+\tau_6\mu_1-\tau_2\mu_5-\tau_5\mu_2)\lambda_1+(\tau_1\tau_6-\tau_2\tau_5)= 0\\
&((\mu_1-\mu_3-\mu_4+\mu_6)\lambda_1+\tau_1-\tau_3-\tau_4+\tau_6)\lambda_2+\\
&\qquad(\mu_1\mu_6-\mu_3\mu_4)\lambda_1^2+(\tau_1\mu_6+\tau_6\mu_1-\tau_3\mu_4-\tau_4\mu_3)\lambda_1+(\tau_1\tau_6-\tau_3\tau_4)= 0
\end{aligned}$$

Eliminating λ_2 yields one polynomial equation of degree 3 in λ_1:

$$\begin{aligned}
&((\mu_1-\mu_2-\mu_5+\mu_6)\lambda_1+\tau_1-\tau_2-\tau_5+\tau_6)\\
&\qquad((\mu_1\mu_6-\mu_3\mu_4)\lambda_1^2+(\tau_1\mu_6+\tau_6\mu_1-\tau_3\mu_4-\tau_4\mu_3)\lambda_1+(\tau_1\tau_6-\tau_3\tau_4))-\\
&((\mu_1-\mu_3-\mu_4+\mu_6)\lambda_1+\tau_1-\tau_3-\tau_4+\tau_6)\\
&\qquad((\mu_1\mu_6-\mu_2\mu_5)\lambda_1^2+(\tau_1\mu_6+\tau_6\mu_1-\tau_2\mu_5-\tau_5\mu_2)\lambda_1+(\tau_1\tau_6-\tau_2\tau_5)) = 0
\end{aligned} \tag{10.9}$$

Solving this equation yields one or three real solutions for λ_1, each of those providing unique values for λ_2, $\mathbf{M}_6$, $\delta^i, i = 1 \ldots 3$ and $\boldsymbol{\mathcal{P}}_i, i = 2, 3$ and thus to 3 different Trifocal tensors using formula (9.12).

The main advantage of this parameterization is that it provides a consistent Trifocal tensor while requiring one point less than the linear method. For this reason, it is a perfect candidate for being the underlying parameterization for a robust algorithm based on e.g. least-median squares (the original work is based on RANSAC). To remove the ambiguity arising from the potentially multiple solutions, the robust criterion is evaluated for all the three tensors and the one providing the smallest result is selected.

10.2.3 The tensorial parameterization

The constraints described by the 9 equations (9.28) can also be used to parameterize the Trifocal tensors with 18 parameters. This parameterization is basically an augmented subset of the Trifocal tensor coefficients, hence the name of tensorial parameterization.

To obtain it, two of the constraints of (9.28) are chosen, for example $k_2 = l_2 = 1,\ k_3 = l_3 = 2$ and $k_2 = l_2 = 2,\ k_3 = l_3 = 3$. Notice that $\boldsymbol{\mathcal{T}}_{.}^{22}$ is the only vector that appears in both constraints. In general, the three vectors $\boldsymbol{\mathcal{T}}_{.}^{23}$, $\boldsymbol{\mathcal{T}}_{.}^{32}$ and $\boldsymbol{\mathcal{T}}_{.}^{33}$ are linearly independent, so that $\boldsymbol{\mathcal{T}}_{.}^{22}$ can be expressed in the basis they form: $\boldsymbol{\mathcal{T}}_{.}^{22} = \alpha_1\boldsymbol{\mathcal{T}}_{.}^{23} + \alpha_2\boldsymbol{\mathcal{T}}_{.}^{32} + \alpha_3\boldsymbol{\mathcal{T}}_{.}^{33}$ Equation (9.28) then implies that $\alpha_1 + \alpha_2\alpha_3 = 0$ It is then easy to parameterize the set of the vectors $\mathcal{T}_{.}^{22}$ that verify the constraint given by $k_2 = l_2 = 2,\ k_3 = l_3 = 3$: $\mathcal{T}_{.}^{22} = \mathbf{K}\,[-pq\ p\ q]^T$, where $\mathbf{K}$ is the matrix $\left[\mathcal{T}_{.}^{23}\ \mathcal{T}_{.}^{32}\ \mathcal{T}_{.}^{33}\right]$. Reporting this value of $\mathcal{T}_{.}^{22}$ in the constraint given by $k_2 = l_2 = 1,\ k_3 = l_3 = 2$, we obtain a polynomial equation P of total degree 4, and of degree 2 in p and q.

The Trifocal tensor can thus be parameterized by 18 parameters. Since there is a global scale factor, one coordinate, e.g. the first coordinate of $\mathcal{T}_{.}^{11}$, can be fixed to be 1. All the vectors $\mathcal{T}_{.}^{11}$, $\mathcal{T}_{.}^{12}$, $\mathcal{T}_{.}^{21}$, $\mathcal{T}_{.}^{23}$, $\mathcal{T}_{.}^{32}$ and $\mathcal{T}_{.}^{33}$ are thus described by 17 parameters. Adding p as the 18th parameter gives a parameterization of the Trifocal tensor. Indeed, then $\mathcal{T}_{.}^{22}$ can be recovered using the polynomial P. Then, as shown in [111], $\mathcal{T}_{.}^{13}$ and $\mathcal{T}_{.}^{31}$ can be recovered up to a scale factor by the formula $(\mathcal{T}_{.}^{12} \times ((\mathcal{T}_{.}^{22} \times \mathcal{T}_{.}^{23}) \times (\mathcal{T}_{.}^{33} \times \mathcal{T}_{.}^{32}))) \times (\mathcal{T}_{.}^{23} \times ((\mathcal{T}_{.}^{22} \times \mathcal{T}_{.}^{12}) \times (\mathcal{T}_{.}^{21} \times \mathcal{T}_{.}^{11})))$ and $(\mathcal{T}_{.}^{21} \times ((\mathcal{T}_{.}^{22} \times \mathcal{T}_{.}^{32}) \times (\mathcal{T}_{.}^{33} \times \mathcal{T}_{.}^{23}))) \times (\mathcal{T}_{.}^{32} \times ((\mathcal{T}_{.}^{22} \times \mathcal{T}_{.}^{21}) \times (\mathcal{T}_{.}^{12} \times \mathcal{T}_{.}^{11})))$, respectively. Each of the remaining scale factors can be recovered using the constraints given by $k_2 = 2,\ k_3 = 1,\ l_2 = 3,\ l_3 = 2$ and $k_2 = 1,\ k_3 = 2,\ l_2 = 2,\ l_3 = 3$, respectively.

It is important to note that, since the polynomial P has to be solved in order to recover the Trifocal tensor, each vector of 18 parameters yields in fact two Trifocal tensors (corresponding to each of the roots of the polynomial). Both tensors are valid: i.e. they verify all the constraints of Trifocal tensors. Thus there is, in general, no way to distinguish between them and both have to be considered: only some extra information can be of some help. This information can be either the image measurements or a boolean describing which of the two roots corresponds to the tensor that has been parameterized. More annoying is the fact that the polynomial P may have no real roots. This shows that the 18 parameters are not totally free but must satisfy an inequality constraint given by the discriminant of P with respect to q. These two drawbacks are particularly annoying if the parameterization is used in a non-linear refinement step.

10.2.4 The minimal univoque parameterization

The final parameterization that is proposed in this section is both minimal and one-to-one. It is based on a parameterization of rank-2 matrices similar to the one used for Fundamental matrices that represent the matrix by its left and right kernels and by a 1-D homography. As shown in the appendix A.2, the space of the 3×3 matrices of rank ≤ 2 having a given left and right kernels, noted $\mathcal{L}$ and $\mathcal{R}$, respectively, is a vector space of dimension 4. We note $\mathcal{M}(\mathcal{L}, \mathcal{R})$ this vector space. We now reformulate the extended rank constraints within this framework.

The 3 matrices $\mathbf{G}^i = \mathcal{T}_i^{..}, i = 1\ldots3$ being rank-2, we note $\mathcal{L}^i$ and $\mathcal{R}^i$ their respective left and right kernels. Each $\mathbf{G}^i$ can thus be represented by its coordinates a_1^i, a_2^i, a_3^i and a_4^i in a basis of $\mathcal{M}(\mathcal{L}^i, \mathcal{R}^i)$. For simplicity, we assume hereafter, without loss of generality, that the first coordinates of $\mathcal{L}^i$ and $\mathcal{R}^i$ are those of highest magnitude, so that we work in the basis described by equation A.3.

Since $\mathcal{L}^i, i = 1\ldots3$ and $\mathcal{R}^i, i = 1\ldots3$ are orthogonal to $\mathbf{e}_{21}$ and $\mathbf{e}_{31}$ respectively, we can write $\mathcal{L}^i = \mathbf{e}_{21} \times \mathbf{X}^{(i)}, i = 1\ldots3$ and $\mathcal{R}^i = \mathbf{e}_{31} \times \mathbf{Y}^{(i)}, i = 1\ldots3$, where $\mathbf{X}^{(i)}$ and $\mathbf{Y}^{(i)}$ are the vectors of formula (9.41).

Plugging these values into the extended rank constraints (9.32)–(9.38) and using computer algebra to factorize the results leads to the following result which is an algebraic translation of proposition 9.15:

Theorem 10.1 *Assuming that the first coordinates of $\mathcal{L}^i$ and $\mathcal{R}^i$ are those of highest magnitude, The four coefficients $a_j^i, j = 1\ldots4$ representing $\mathbf{G}^i$ in $\mathcal{M}(\mathcal{L}^i, \mathcal{R}^i)$ satisfy the following* linear *relation:*

$$e_{21}^2 e_{31}^2 a_1^i + e_{21}^2 e_{31}^3 a_2^i + e_{21}^3 e_{31}^2 a_3^i + e_{21}^3 e_{31}^3 a_4^i = 0\ , \tag{10.10}$$

where $\mathbf{e}_{21} = \left[e_{21}^1, e_{21}^2, e_{21}^3\right]^T$ and $\mathbf{e}_{31} = \left[e_{31}^1, e_{31}^2, e_{31}^3\right]^T$.

Remark 10.1

- *Equations 10.10 are only factors that appear in the extended rank constraints, but it can be shown that they are the only one that must generically vanish.*
- *In the general situation, the first coordinates of $\mathcal{L}^i$ and $\mathcal{R}^i$ are not those of highest magnitude. It is remarkable to note that equation (10.10) remains essentially the same with the substitution of e_{21}^j and e_{31}^k by $e_{21}^{\lambda^i(j)}$ and $e_{31}^{\rho^i(k)}$, where λ^i and ρ^i are the circular permutations that bring respectively the coordinates of highest magnitude of $\mathcal{L}^i$ and $\mathcal{R}^i$ into first position. This is quite remarkable as the original constraints all depend on at least two of the three $\mathbf{G}^i, i = 1\ldots3$.*
- *It is not difficult to show that equations (10.10) are never degenerated provided that the proper permutations λ^i and ρ^i have been made.*

Assuming first that the 6 vectors $\mathcal{L}^i, i = 1\ldots3$ and $\mathcal{R}^i, i = 1\ldots3$ are given, the three matrices $\mathbf{G}^i, i = 1\ldots3$ can be parameterized by 8 coefficients. To do so, consider the 12 coordinates $a_j^i, i = 1\ldots3, j = 1\ldots4$. Since for each i the $a^i_j, j = 1 \dots 4$ are satisfying equation (10.10), it is possible to drop one of those four coordinates: for numerical stability, the best choice is to drop the coordinate which has the highest coefficient in magnitude in equation (10.10). Moreover, since the $\mathbf{G}^i$ are only defined up to a global scale factor, we can drop one more of the 9 remaining coordinates by normalizing it to 1. This leaves us with 8 coefficients that completely describe the $\mathbf{G}^i, i = 1 \dots 3$, given the $\boldsymbol{\mathcal{L}}^i, i = 1 \dots 3$ and $\boldsymbol{\mathcal{R}}^i, i = 1 \dots 3$.

Since 8 parameters have been used, only 10 parameters remain to parameterize the $\boldsymbol{\mathcal{L}}^i, i = 1 \dots 3$ and $\boldsymbol{\mathcal{R}}^i, i = 1 \dots 3$. We next show that 5 parameters are enought to parameterize e.g. the $\boldsymbol{\mathcal{L}}^i, i = 1 \dots 3$ (since a similar parameterization can be obtained for the $\boldsymbol{\mathcal{R}}^i, i = 1 \dots 3$, a minimal parameterization of the Trifocal tensor is thus obtained). $\mathbf{e}_{21}$ can be parameterized by 2 coordinates by normalizing its biggest coordinate to 1 (there are thus 3 maps). Assuming without loss of generality that $\|\boldsymbol{\mathcal{L}}^i\| = 1, i = 1 \dots 3$, and remembering that all these 3 vectors are orthogonal to the epipole $\mathbf{e}_{21}$, the 3 vectors $\boldsymbol{\mathcal{L}}^i$ are conveniently represented by 3 angles in a canonical basis of the plane orthogonal to the direction defined by $\mathbf{e}_{21}$. Thus, all the $\boldsymbol{\mathcal{L}}^i$ can be represented by 5 parameters.

As a consequence, we have obtained a minimal parameterization of the Trifocal tensor, i.e by 18 parameters. As the reader may have noticed, the number of maps of this parameterization is very large ($9 \times 3^2 \times 3^6$) but it is nonetheless easy to define a general routine that chooses the best map and computes the parameterization.

10.3 Imposing the constraints

Since a Trifocal tensor $\widehat{\boldsymbol{\mathcal{T}}}$ obtained from the linear method is not consistent (ie does not satisfy the Trifocal constraints), parameterizing such a tensor involves first a procedure that enforces the consistency. As in the Fundamental matrix case, this is usually (if not always) done considering only the obtained Trifocal tensor (ignoring the primitive matches that led to its computation). Consequently, this crucial step to most Trifocal tensor estimation methods can introduce a significant decrease in the quality of the solution with respect to the data. The operation is nonetheless mandatory. To impose the constraints, two routes can be taken:

- Define a robust version of the procedure that computes one of the parameterizations of the previous section from a tensor. Then, resynthetize the Trifocal tensor from this parameterization. The tensor obtained this way will be consistent.

- Use the formulae of the Trifocal constraints to define a projection method that takes a point in a 27 dimensional space (the space of all $3 \times 3 \times 3$ tensors) onto the variety of dimension 18 defined by those constraints (the variety of the admissible tensors).

The next two sections illustrate these basic approaches. A third section compares the results obtained with those.

10.3.1 Projecting by parameterizing

Some of the parameterizations defined in the previous section can lead to very simple procedures that can be used to impose the constraints. This is particularly the case with the parameterization by projection matrices (see section 10.2.1) and with the minimal one (see section 10.2.4)[4], which are taken here as examples.

Both parameterizations are based on the knowledge of the epipoles, so the first step is to estimate these out of a non-consistent tensor. This can be done very easily by considering the 3 matrices $\widehat{\mathbf{G}}^i = \widehat{\mathcal{T}}_i^{jk}, i = 1 \ldots 3$. Since these should be of rank 2, the first step is to enforce this constraint, which can easily be done using the closest rank method described in section 7.2.3. Equipped with the new rank-2 versions $\widehat{\mathbf{G}'}$ of these matrices, it is now possible to extract their left and right kernels $\widehat{\mathcal{L}'}^i, i = 1 \ldots 3$ and $\widehat{\mathcal{R}'}^i, i = 1 \ldots 3$ as in section 10.2.4. Because of proposition 9.19, we also know that the matrices $\widehat{\mathcal{L}'}$ and $\widehat{\mathcal{R}'}$ whose columns are respectively the $\widehat{\mathcal{L}'}^i$ and the $\widehat{\boldsymbol{R}'}^i$ should also be of rank 2 and that their kernels correspond to $\mathbf{e}_{21}$ and $\mathbf{e}_{31}$ respectively. Using a least squares method to get these kernels gives estimations $\widehat{\mathbf{e}_{21}}$ and $\widehat{\mathbf{e}_{31}}$ of the epipoles.

Once estimations of the epipoles have been recovered, the methods for the two kinds of parameterizations follow different paths:

- For the parameterization by projection matrices, it is sufficient to solve the system 10.8 using least-squares to find values for the α_j^i and β_j^i co-

[4]Being based on a very different kind of input, the six point parameterization is more difficult to use in this context. Given a non-consistent Trifocal tensor, it should be possible, in theory, to use it to define a set of 6 point matches for the three images, and to excerpt a consistent tensor out of this description. The choice of the 6 points is, however, non-obvious.

efficients ($i = 1 \ldots 3, j = 1 \ldots 3$). It is possible to make this estimation while enforcing the constraint $\sum_i \alpha_j^i \alpha_4^i = 0$.

- For the minimal parameterization, it is sufficient to solve the equation $\widehat{\mathbf{G}}^i = a_1^i \mathbf{M}_1^i + a_2^i \mathbf{M}_2^i + a_3^i \mathbf{M}_3^i + a_4^i \mathbf{M}_4^i$ ($\mathbf{M}_j^i, i = 1 \ldots 3, j = 1 \ldots 4$ is the basis taken for $\mathcal{M}(\widehat{\boldsymbol{\mathcal{L}}'}^i, \widehat{\boldsymbol{\mathcal{R}}'}^i)$) imposing the constraint (10.10).

In both cases, taking the image information during this last step is possible. The method for the parameterization by projection matrices case be found as a by-product of Hartley's method [150].

10.3.2 Projecting using the algebraic constraints

Alternatively, it is also possible to develop a minimization scheme directly based on the Trifocal constraints. To do so, one just minimizes the residual of the algebraic constraints over the coefficients of the Trifocal tensor. The mere advantage of this method is that potentially all constraints are treated on the same level. Looking back at what has been described in the previous section, we see that the various constraints are enforced in a hierarchical way: first the rank constraints of the matrices $\mathbf{G}^i$ are enforced, then the Trifocal epipolar constraints are taken into account and the final step (whatever the parameterization) enforces the remaining constraints.

One advantage of the scheme based directly on the Trifocal constraints is that it is possible in theory to handle all the constraints at the same level. Thus, potentially, the magnitude of the changes of the coefficients of the Trifocal tensor required to impose the constraints is smaller. However, the high degree of some formulations of the constraints (e.g. those of equation (9.28)) imposes some modifications to this simple scheme in order to obtain convergence of the minimization procedure (ie avoid to stay trapped on some local minimum). In [113], this is obtained by dealing with the rank constraints of the matrices $\mathbf{G}^i$ separately. This is still one level of hierarchy less than the methods using parameterization but reduces nonetheless the main interest of such methods. There is hope, however, as the extended rank constraint (see proposition 9.20) are of much lower degree and are thus much less prone to induce local minima. Initial results show that the convergence is much better when using the method described in [113] with these constraints, so that supressing the hierarchy has very good chances to work.

One fact remains: in all cases, the image data are ignored when applying these methods and this is bad since these data are the only relevant metric that can be used to measure the quality of the computed Trifocal tensor (ie its accuracy in describing the image data). Conceptually, it is possible to design a constrained least-squares minimization that will deal with this problem, we have to remember, however, that imposing constraints is just a step needed for a full non-linear algorithm which will handle this problem in a much better way.

10.3.3 Some results

We now examin the effect of imposing the Trifocal constraints on the results obtained in the experiments of section 10.1.4.2. For each of these experiments, the result of the linear estimation has been used as the input of the following projection methods:

P1 The projection by parameterization method using the parameterization by projection matrices.

P2 The projection by parameterization method using the minimal parameterization.

P3 The algebraic projection method sketched in section 10.3.2 based on the extended rank constraint.

In each case, the geometric errors between the data points and the predicted ones are shown in table 10.3. For reference, the results obtained with the linear estimation of the Trifocal tensor (which is the initial input provided to the various projection methods) is shown as the experiment **P0**. In this case, the change of view operation leads to a non-coherent over-determined linear system which is solved using a least-squares technique. As it can be seen, even though the geometric residuals remain small in image 1, those obtained in such a way in images 2 and 3 can be very large.

From these results, several observations can be made:

- For all the projection methods, the geometric errors in image 1 somewhat increase during the projection operation. On the other hand, the residual geometric errors in images 2 and 3 are considerably decreased.

- The methods P1 and P2 basically behave the same way, with P1 consistently giving slightly better results than P2.

		Office		Office'		Library		Library'		Arcades	
		Average	Max	Average	Max	Average	Max	Average	Max	Average	Max
	Image 1	1.6	4.3	1.4	3.7	2.3	9.3	0.5	2.5	0.8	2.0
2- P0	Image 2	4460.6	29711	7794.8	100626	32.0	81.7	1.8	4.9	259.9	546.4
2-	Image 3	876.6	5209.4	842.4	1436	334.0	1964.1	21.1	84.9	214.8	720.2
	Image 1	2.2	8.4	2.7	11.7	3.0	10.6	1.0	5.4	2.9	10.1
2- P1	Image 2	4.9	18.9	5.4	21.9	1.6	3.8	0.6	1.7	1.1	3.6
2-	Image 3	5.6	32.5	5.4	28.7	0.9	3.0	0.4	1.6	2.7	8.3
	Image 1	2.3	9.3	2.9	14.9	4.4	24.7	1.5	7.4	3.4	10.7
2- P2	Image 2	5.7	24.2	6.5	29.0	1.5	4.0	0.6	1.6	1.3	3.5
2-	Image 3	6.7	38.8	6.9	36.8	1.1	2.8	0.4	1.7	2.7	6.6
	Image 1	3.3	17.8	3.1	18.8	2.7	10.6	1.0	4.6	1.5	4.3
2- P3	Image 2	3.0	8.7	2.9	10.5	1.3	4.6	0.5	1.4	0.6	1.2
2-	Image 3	4.5	21.3	4.6	18.8	0.8	2.6	0.4	1.7	1.6	3.4

Table 10.3: Quality of the various projection methods with real data. For each experiment, the average and maximum error is given. For reference, the experiment P0 corresponds to the initial results provided to the projection method : these are the results of the linear method. Because the trifocal constraints are not satisfied, a robust version of the change view operation has been used.

- The method P3 does a better jobs in homogeneizing the error patterms over the 3 cameras. This is sometimes at the cost of increasing more the geometric errors in image 1 than the methods P1 or P2.
- All the methods presented here tend to work much better when applied to the tensor written in normalized coordinates (see 10.1.1).

In all these cases, the resulting geometric errors – particularly the maximum errors – remain innacceptably large considering that the initial matching has been done manually on images of good quality (so that the maximum error should not exceed 3–5 pixels).

10.4 A note about the "change of view" operation

The change of view operation is important as it is the procedure that will allow for a symmetrical estimation of all the three tensors associated to three views. This operation can be achieved in three ways:

- Use theorem 9.2: however as given the theorem is not explicit as no expressions are given for the values λ_m, $m = 1, 2, 3$. This lack of values actually corresponds to the fact that no expression that is always valid has been found yet. For this reason, it seems unsafe to use this approach.
- Directly use equation $\mathbf{l}_j \simeq \boldsymbol{\mathcal{T}}_j(\mathbf{l}_k, \boldsymbol{\mathcal{T}}_i(\mathbf{l}_j, \mathbf{l}_k))$ that is true for all possible values of $\mathbf{l}_j$ and $\mathbf{l}_k$: when developped and organized as a polynomial in the coordinates of $\mathbf{l}_j$ and $\mathbf{l}_k$, this equation has 90 terms each of which has a coefficient which is linear in the coefficients of $\boldsymbol{\mathcal{T}}_j$ and in the coefficients of $\boldsymbol{\mathcal{T}}_i$ and must be zero. Removing the equations that appear multiple times, this gives a linear system of 54 equations in the 27 unknowns relating $\boldsymbol{\mathcal{T}}_j$ to $\boldsymbol{\mathcal{T}}_i$. With consistent tensors, this system is of rank 26 and has a non-trivial solution. With non-consistent tensors, a least-squares solution of the system can be used.
- Using the parameterization by projection matrices described in section 10.2.1, it is possible to re-synthesize all the three Trifocal tensors corresponding the the three views using the formula (9.12). If the initial tensor is not consistent, then the method sketched in section 10.3.1 can be used to get the parameterization.

The last two methods are both valid and give the same results in the case of a consistent tensor. In the case of a non consistent tensor, however, the least-squares implementations of these methods will give different solutions: for example, the method using the projection by projection matrices will always yield a consistent tensor as a result; this is not the case with the method based on the linear system. On the other hand, this last method should provide a solution that minimizes the algebraic error of the system characterizing the change of view operation, which cannot be claimed with the parameterization based method. This is stronly related to the topic discussed in section 10.3.

10.5 Non-linear methods

The linear method described in section 10.1 has the main advantage of being easy to implement and of defining the Trifocal tensor as the unique minimum of a convex criterion. However, it suffers also of some structural and numerical limitations:

- It is based on an algebraic criterion, which is only loosely related to the more natural geometric criterion that defines the error between the measures and the predicted primitives (from the other views) in terms of image distances.
- It minimizes a criterion that is biased: the Trifocal tensor $\mathcal{T} = \mathcal{T}_1$ gives a special role to image 1. Consequently, the criteria that have been defined in section 10.1 are not symmetric with respect to the primitives of the three images (contrarily to what happens in the Fundamental matrix case). In particular, we have seen that the linear method cannot use the information available from the matches of type line-point-line or line-line-point or line-point-point.
- The Trifocal constraints are not satisfied by the solution obtained using the linear estimation since it assumes that all the 27 parameters of the tensor are independant. With perfect data this is not a problem as the computed tensor will be very close to the real solution and hence the constraints will be satisfied. With noisy data, this is no longer the case.

Non-linear methods can take care of these limitations at the cost of introducing local minima. On the other hand, there is usually no explicit way of finding the global minimum and non-linear methods use iterative schemes that are highly sensitive to the initialization. Thus, as for the Fundamental matrix computation, the usual strategy is to initialize a non-linear method with the result of the linear one (assuming that this result is close to the non-linear optimum).

10.5.1 The non-linear scheme

To achieve the non-linear minimization, the main ingredients are:

- **A geometric criterion**, that will characterize the quality of the estimation and that will be minimized in order to refine the estimated Trifocal tensor.
- **A method for projecting** an initial tensor not satisfying the Trifocal constraints onto a "feasible" tensor.
- **A parameterization** of the Trifocal tensor: this is needed to ensure that the non-linear optimization method "explores" only the feasible situations, ie those that are satisfying the Trifocal constraints.
- **The "change of view" operation**: this tool is needed to make the estimation procedure symmetric with respect to all the images.

The general scheme is the following:

1. Compute an initialization $\widehat{\boldsymbol{\mathcal{T}}}$ of the Trifocal tensor using the linear method (see section 10.1).
2. Project this tensor $\widehat{\boldsymbol{\mathcal{T}}}$ to obtain a consistent tensor $\overline{\boldsymbol{\mathcal{T}}}$ (see section 10.3) and parameterize the tensor using one of the parameterizations of section 10.2. As seen in section 10.3 these two steps can sometimes be combined. This gives a 18 parameters vector $\mathbf{p} = \mathbf{p}_0$ describing $\overline{\boldsymbol{\mathcal{T}}}$.
3. Use an iterative algorithm to refine $\mathbf{p}$ so as to minimize a geometric criterion defined as:
   - Recover $\overline{\boldsymbol{\mathcal{T}}} = \overline{\boldsymbol{\mathcal{T}}_1}$ from $\mathbf{p}$ (see section 10.2)
   - From $\overline{\boldsymbol{\mathcal{T}}_1}$, compute $\overline{\boldsymbol{\mathcal{T}}_2}$ and $\overline{\boldsymbol{\mathcal{T}}_3}$ using the "change view" operation (see section 10.4).
   - Sum up the geometric errors arising from $\overline{\boldsymbol{\mathcal{T}}_1}$, $\overline{\boldsymbol{\mathcal{T}}_2}$ and $\overline{\boldsymbol{\mathcal{T}}_3}$ to obtain a criterion that is symmetric over the three views.

Note that overall this method is very similar to what does a bundle adjustment procedure. Some variants of this basic algorithm have been explored:

- The 6 points parameterization can be used as a replacement of steps 1 and 2. Six initial point matches are randomly chosen from the input data to obtain an initial consistent Trifocal tensor. A robust criterion is then used to estimate the quality of the tensor with respect to all the primitives. By iterating over the choice of the initial points this leads to a method that deals with outliers. The main drawback of this method, is its restriction to use solely point matches for the initial parameterization which is somewhat restrictive if the input consists essentially in line matches. See [371] for more details.

- Dropping the symmetry over the three views (ie minimizing only the errors arising from eg $\mathcal{T}_1$) and replacing the geometric criterion by the algebraic one (the one minimized by the linear method) and using the parameterization by projection matrices, it is possible to design a simpler estimation procedure for which the non-linear optimization is used to refine only the epipole positions, the remaining parameters being estimated linearly using equation 10.8. See [140] for more details.

10.5.2 A note about the geometric criterion

Up to now, we have omitted the details of the geometric criterion. Basically, the geometric criterion is very similar to the one used for the Fundamental matrix. The only difference here is that we have to deal with both lines and points. The situation is the following:

- In each image, the inputs are points and line-segments.

- The prediction obtained by the Trifocal tensor in one view given the primitives in the two other views is either a point or an infinite line.

Thus, if we want to deal with all these types of primitives, we need to define and combine all the geometric distances from an image feature to a predicted feature. The point-point and point-line distances are well known, but the distances from a line-segment to a point or a line require some attention. Let us call $\mathbf{s}$ the line-segment and $\mathbf{a}$ and $\mathbf{b}$ its end-points.

The distance of a point m to the line segment s is very similar to the point-line distance. Denoting by $\mathbf{l}$, the support line of $\mathbf{s}$, one just has to pay attention to the end-points of the segment. Two cases are possible:

- The projection of $\mathbf{m}$ onto $\mathbf{l}$ lies on $\mathbf{s}$, then the distance between $\mathbf{m}$ and $\mathbf{s}$ is simply the distance between $\mathbf{m}$ and $\mathbf{l}$.
- The projection of $\mathbf{m}$ onto $\mathbf{l}$ does not lie on $\mathbf{s}$, then the distance between $\mathbf{m}$ and $\mathbf{s}$ is the smaller of the two distances between $\mathbf{m}$ and $\mathbf{a}$ and $\mathbf{b}$ respectlively.

The distance of a line-segment to a line l is slightly more complicated to define. Many definitions can be adopted: one solution very often taken is to sum up the distances of the two end-points to the line. This is indeed a proper distance in mathematical terms. However, since we are combining very different error terms, we also want that the various distances that we are summing up are weighted homogeneously over the various primitives (ie a segment of length l has the importance of roughly l points). Thus, the only way to define properly this distance is to sum up the contributions of all the points of the line-segment to the distance to the line $\mathbf{l}$. This is done by integrating the squared distance of $\mathbf{m}$ to $\mathbf{l}$ for every point $\mathbf{m}$ of $\mathbf{s}$, and taking the square root of this value. This computation can be made algebraically and the result is:

$$d(\mathbf{s}, \mathbf{l}) = \sqrt{d(\mathbf{a}, \mathbf{b}) \left(\frac{(\mathbf{u}^T\mathbf{a} - \mathbf{u}^T\mathbf{b})^2}{3} + d(\mathbf{a}, \mathbf{l}) d(\mathbf{b}, \mathbf{l}) \right)} \; .$$

where $\mathbf{u}$ is the normalized vector describing the normal to the line $\mathbf{l}$.

10.5.3 Results

We now examin the behaviour of the non-linear methods on the results obtained in the experiments of section 10.1.4.2. For each of these experiments, the result of the linear estimation has been used, then the algebraic projection methods has been applied to obtain an initial tensor satisfying the trifocal constraints. This tensor is parameterized and used as the initial solution in non-linear estimation techniques. Basically, two types of parameterizations have been used:

P: The parameterization by projection matrices.

M: The minimal parameterization.

		Office		Office'		Library		Library'		Arcades	
		Average	Max	Average	Max	Average	Max	Average	Max	Average	Max
	Image 1	3.3	17.8	3.1	18.8	2.7	10.6	1.0	4.6	1.5	4.3
2- P3	Image 2	3.0	8.7	2.9	10.5	1.3	4.6	0.5	1.4	0.6	1.2
2-	Image 3	4.5	21.3	4.6	18.8	0.8	2.6	0.4	1.7	1.6	3.4
	Image 1	1.5	3.8	1.4	4.1	1.5	4.3	0.3	0.6	0.9	1.8
2- P	Image 2	2.2	5.2	2.1	5.2	1.2	4.1	0.2	0.4	0.5	1.1
2-	Image 3	2.3	7.8	1.9	5.8	0.9	2.1	0.2	0.8	0.9	2.4
	Image 1	1.7	5.4	1.6	4.4	1.5	4.7	0.3	0.6	0.9	2.8
2- M	Image 2	2.3	5.6	2.2	5.2	1.2	3.7	0.2	0.4	0.5	1.0
2-	Image 3	2.7	9.0	2.3	7.6	0.8	2.0	0.1	0.8	1.0	2.4

Table 10.4: Quality of the non-linear estimation of the Trifocal tensor with real data. For each experiment, the average and maximum error is given. For comparison puposes, the results obtained before non-linear refinement are shown : these are the results obtained in the P3 experiment given in section 10.3.3.

However, it should not be forgotten that the Trifocal tensor is a non-symmetric object across the three views. This property is also true of the two above types of parameterizations since each of these attribute a special role to one of the cameras. Thus by changing views, each of these parameterization types is actually giving three parameterizations for a single Trifocal tensor. Numerically, one indeed notices that, for a given type of parameterization, the three possible parameterization are not giving the same results. This is all the more important as it seems that the local minima of the minimized criterion is highly dependent on the parameterization. Consequently, in order to avoid to remain trapped in those local minima, the non-linear optimization procedure is applied using in sequence each of the three parameterizations. This has also the nice effect of making the non-linear procedure as symmetric as possible over the three views.

In each case, the geometric errors between the data points and the predicted ones are shown in table 10.4. For reference, the results obtained with the initial Trifocal tensor used as input to the non-linear methods is shown as the experiment **P3**.

As it can be seen from the results, the non-linear estimations improve quite a lot the quality of the estimations of the Trifocal tensors, decreasing dramatically the maximum errors. Still, these results are not yet perfect as the maximum errors are still too high. Indeed, it seems that these solutions often correspond to situations close to a local minimum with a narrow and flat valley leading to a better solution at very slow speed.

Another interesting fact is that as for the projection methods, it seems that the parameterization by projection matrices performs better than the minimal parameterization. Althought, no real explanation can be given at the time of this writing, it seems to be related with the fact that the parameterization by projection matrices is "more linear" than the minimal parameterization which involves trigonometric functions.

Figure 10.5: Three views of the INRIA library (Courtesy **Sylvain Bougnoux**, INRIA). These data correspond to the **Library** and **Library'** experiments.

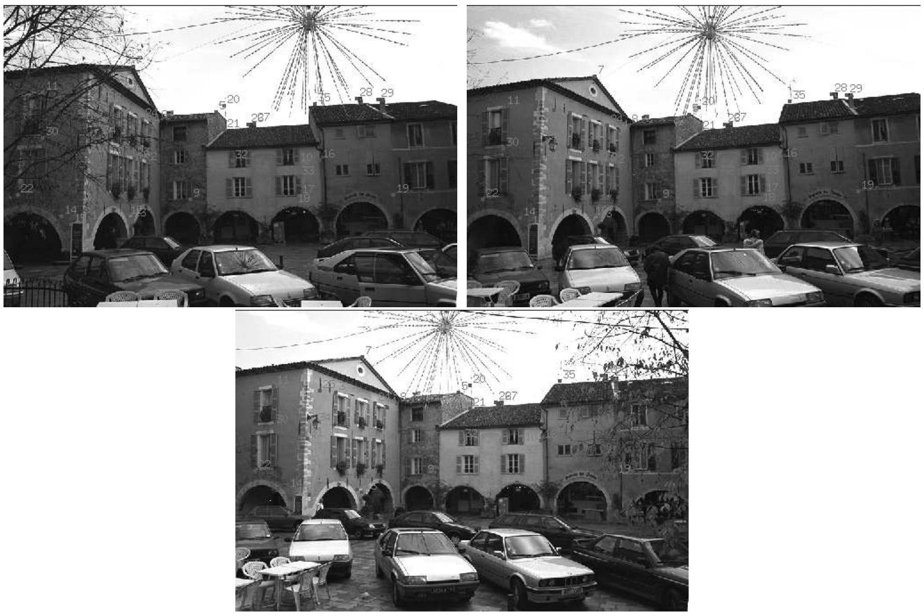

Figure 10.6: Three views of the Arcades square in Valbonne (Courtesy **Sylvain Bougnoux**, INRIA). These data correspond to the **Arcades** expriment.